Ultra-Compact Bragg-Assisted Silicon Photonics Orbital Angular Momentum Emitter

F. Gambini[(1)], Y. Liu[(1)], B. Song[(1)], H. Zhao[(1)], V. Rosborough[(1)], F. Sang[(1)], P. Velha[(2)], S. Faralli[(2)], J. Klamkin[(1)]
[(1)]*Electrical and Computer Engineering Department, University of California, Santa Barbara, CA 93106, USA*
[(2)]*Scuola Superiore Sant'Anna, via G. Moruzzi, 1, 56124, Pisa, Italy*
fgambini@ucsb.edu

Abstract: An ultra-compact microring-based Orbital Angular Momentum (OAM) emitter is demonstrated for free-space optical communications. The device relaxes the fabrication constraints and enables fast OAM switching and multiple OAM modes at the same wavelength.
OCIS codes: 130.0130, 250.5300.

1. Introduction

The spectral efficiency [1-4] and security [5], of the future reconfigurable high-speed [2] free-space and wireless optical communication systems, could be strongly improved by the properties of mutually OAM modes [1]. OAM provides additional data carrier dimension with reduced crosstalk, high multiplexing and de-multiplexing efficiency and theoretically infinite number of OAM states supported by a single light beam [3]. Compact, fast, reconfigurable and high efficiency devices are required for large scale integration wavelength division multiplexing (WDM) systems. The viability of integrated reconfigurable ring-based OAM emitters has been demonstrated by Strain et al. [6]. Although it exhibits high switching speed and thermal efficiency, fabrication constraints are introduced by the use of a 300-nm thick silicon dioxide layer.
This work, based on previous results [7] and theoretical analysis [8], experimentally demonstrates the performance of fast thermally tunable OAM emitter, based on a 10-µm radius ring resonator in silicon-on-insulator (SOI) platform, for vertical emission of radially-polarized OAM modes. The device supports multiple OAM states at the same operating wavelength exploiting an alternative design using holes instead of angular gratings [8] and an integrated conducting path. The fabrication constraints for the SOI platform are relaxed despite the ultra-compact footprint and the limited optical loss.

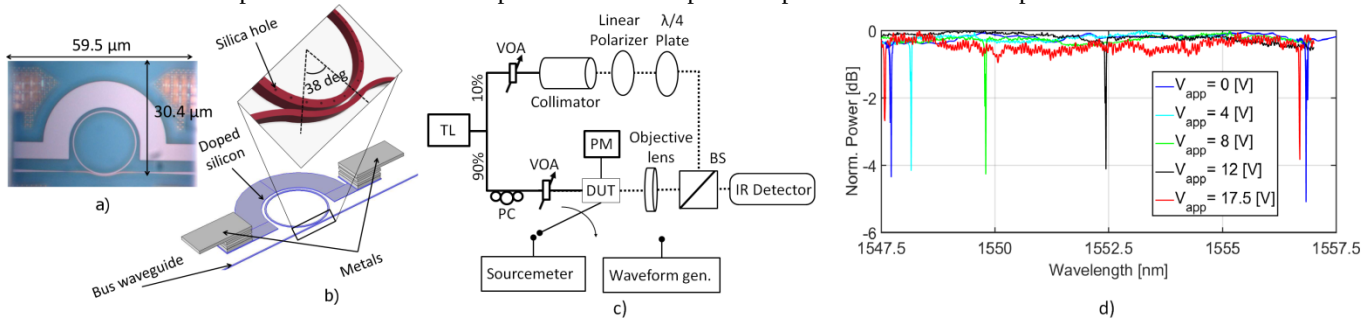

Fig. 1. Device microscope image of the realized OAM emitter a), scheme b), experimental setup c) and resonance tuning of the ring for different applied voltage d).

2. Device design

The device consists of an integrated heater, based on a high-doped silicon circular ridge, which surrounds a single 10-µm radius silicon microring. Finite-difference time-domain [9] and multiphysics simulations [10] were used for electromagnetic and thermal analysis, respectively. The microring resonator is a single-mode 500x220 nm^2 transverse-electric (TE) silicon waveguide with 69 fully-etched cylindrical holes periodically placed along its central path. This distributed Bragg grating is composed of 50-nm radius holes and filled with silica. The ring resonator has been designed in order to emit around 1555 nm an OAM with topological charge [1] *l=1*. The inter-waveguide gap between the bus and the ring is limited, due to technological constraints, to 100 nm. In order to optimize the coupling coefficient between the bus and the ring, the waveguide width of the bus is set to 300 nm and the bus is bent by an optimized angle of 38 degrees in the coupling region. The 220-nm thick and 8.5-µm wide integrated resistive heater is composed of highly doped silicon and it is located 1 µm far from the silicon ring, in order to minimize the optical loss. The resonant wavelength is changed exploiting the Joule effect by controlling the injected electrical current. The footprint of the device is about 30.4x59.5 µm^2 and the photonic integrate circuit (PIC) was manufactured in a multi-project wafer run. In Fig. 1 a) the microscope image of the realized device is reported while in Fig. 1 b) the schematic of the device is shown.

3. Experimental results

The setup shown in Fig. 1 c) was used to test the performance of the PIC. A homodyne interferometer was built in order to detect the emitted OAM state. A continuous wave signal with 5 dBm of optical power was generated by an external cavity tunable laser

(TL) and swept from 1535 to 1570 nm. A 90/10 optical splitter divides the signal in two arms. In the lower arm a polarization controller (PC) maximizes the coupling efficiency between the fiber and on-chip edge coupler. In the upper arm a collimator generates a free-space Gaussian-like beam. A linear polarizer and a quarter-wave plate convert the mode to a left- or right-handed circularly polarized (LHCP and RHCP, respectively) reference beam. An electrical sourcemeter or waveform generator, electrically connected with the integrated heater, have been used to tune the resonant wavelength of the device under test (DUT). At the top of the DUT, an objective lens collects the vertically emitted beam while a free-space 3-dB beam splitter (BS) combines the two signals. The power unbalanced due to different propagation loss in the two arms are equalized using variable optical attenuators (VOAs). An infrared (IR) camera detects the output signal, while, an optical powermeter (PM) evaluates the output optical power at the through-port of the device. Fig. 1 d) reports the normalized spectra at different applied voltages, from 0 to 17.5V. The free spectral range (FSR) is about 9.2 nm at 0V. Due to high bus-ring waveguide coupling coefficient the extinction ratio of the notches are limited to 5 dB. This also reduces the emission efficiency which is less than 1%. In the future, an optimized design of the coupler will improve the emission efficiency of the device. The heater resistance is 1.5 kΩ. The goal of 97 mW/FSR was not achieved due to fabrication inaccuracies that degraded the thermal tuning efficiency [8], however, the tunability has been demonstrated up to one FSR between T0 = 22 °C and T1=T0+127 °C. The measured emitted OAM LHCP phase patterns for l=+3 (a), +2 (b), +1 (c) and 0 (d) at T0 and l=+4 (e), +3 (f), +2 (g) and +1 (h) at T1 are shown in Fig. 3. The number of arms in the spirals are clearly visible and equal to l-1. Despite the small discrepancies related to fabrication and tuning inaccuracies, Fig. 3 demonstrates that the device supports multiple OAM modes. In order to prove that the device also supports RHCP OAM modes, RHCP far-field phase patterns are reported for l=+1 (i) and 0 (j) at T0 and l=+2 (k) and +1 (l) at T1. Fig. 3 m) shows the switching time of the device for dynamic tuning of the OAM states. A voltage impulse has been applied and the optical response has been recorded and fitted with a first order response:

$$\frac{\Delta T}{T_{max}} = 1 - exp\{-t/\tau\} \quad (1)$$

where τ is the switching time constant and it is equal to 19.5 µs, which is close to the multiphysics simulation result: 17 µs.

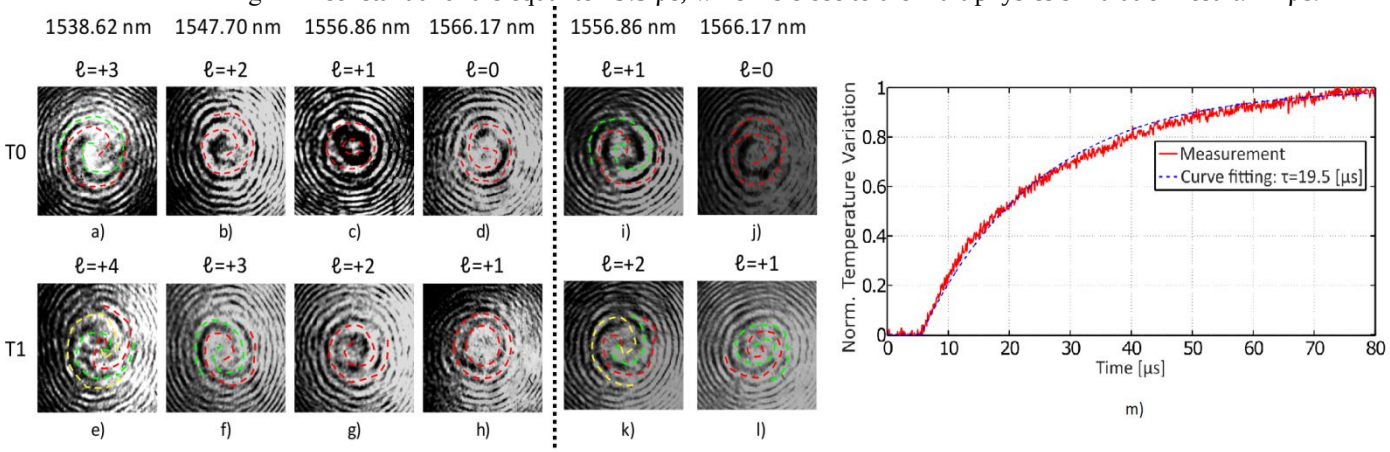

Fig. 3. Far-field intensity patterns for LHCP a)-h) and RHCP i)-l) OAM modes at temperature T0=22 °C and T1=T0+127 °C and measured switching time response (continuous red) and first order curve fitting (dashed blue) m).

4. Conclusions

A fast ultra-compact integrated silicon microring-based Bragg-assisted OAM emitter has been experimentally demonstrated. The alternative design allows to relax the fabrication constraints and allows the generation of multiple RHCP and LHCP radially-polarized OAM modes at the same wavelength. The far-field phase patterns are plainly visible and the switching time of the device is 19.5 µs.

5. References

[1] Allen L. et al., "Orbital angular momentum of light and the transformation of Laguerre-Gaussian laser modes," Phys. Rev. A, 45, 11, 8185 (1992).
[2] H. Zhao et al., "Indium Phosphide Photonic Integrated Circuits for Free Space Optical Links," IEEE J. Sel. Topics Quantum Electron., 24, 6, 1-6 (2018).
[3] A. E. Willner et al., "Optical communications using orbital angular momentum beams," Adv. Opt. Photon., 7, 66 (2015).
[4] D. Zhang et al., "Encoding and decoding of orbital angular momentum for wireless optical interconnects on chip," Opt. Express, 20, 26986 (2012).
[5] M. Mirhosseini et al., "High-dimensional quantum cryptography with twisted light," New J. Phys., 17 33033 (2015).
[6] M. J. Strain et al., "Fast electrical switching of orbital angular momentum modes using ultra-compact integrated vortex emitters," Nat. Comm., 5, 4856 (2014)
[7] F. Gambini et al., "Orbital angular momentum generation with ultra-compact Bragg-assisted silicon microrings," Photon. Technol. Lett., 28, 21, 2355 (2016)
[8] F. Gambini et al., "Design of an integrated Bragg-assisted tunable silicon microring for orbital angular momentum generation," in Proc. Advanced Photonics, ITu3B.4., Vancouver, (2016)
[9] Lumerical Solutions, Inc., Innovative Photonic Design Tools, www.lumerical.com.
[10] COMSOL Multiphysics, www.comsol.com.